DESERTIFICATION PHENOMENON ASSESSMENT IN AL-HAY DISTRICT, WASIT/IRAQ USING REMOTE SENSING TECHNIQUES

Ammar A. Jasim[1], Mahir M. Hason[1], Awad A. Sahar[2] and Talal Hasan Kadhim[3*]

[1] Scientific Research Commission, Ministry of Higher Education and Scientific Research , Baghdad, Iraq;
 e-mail: dr.ammarabd77@mohesr.edu.iq ; dr.mahir.mahmod@src.edu.iq

[2] Department of Chemical Engineering and Oil Refining, Kut University College, Wasit, Iraq;
 e-mail: Awad.Sahar@alkutcollege.edu.iq

[3] Department of Geology, College of Science, University of Baghdad; e-mail: talalkazem@yahoo.com

* *Corresponding author email: talalkazem@yahoo.com ; ORCID: 0000-0002-2024-3400)*

Abstract

Desertification has developed rapidly in recent years due to years of neglect in environmental management, especially in the agriculture and irrigation sectors in the study area (Al-Hay District, Wasit Governorate, Iraq). Several factors have combined to create this problem within the lands of the study area, represented by natural geographical factors, such as climate, soil, water, and natural vegetation. Therefore, it has become necessary to address the phenomenon of desertification in this work, especially after waves of water scarcity, problems of human urban expansion, and droughts that have swept many countries. The current research aims to evaluate the desertification phenomenon by monitoring the changes in the land cover and land use of the study area, as an attempt to develop solutions and proposals that may contribute to the process of reducing the spread of desertification. Integration between remote sensing (RS) techniques and geographic information systems (GIS) is utilized to evaluate desertification and assess the sensitivity of areas to this phenomenon that traditional methods (e, g. direct observation, map interpretation, and field survey) are unable to provide. Supervised and unsupervised classification techniques were utilized to build a geographic information base by analyzing and interpreting the satellite images of the Landsat 8 satellite. The findings demonstrated how crucial it is to integrate RS and GIS while tracking the desertification phenomenon, both inside and outside of the study area. The categorized images are considered appropriate for further research because Kappa coefficients are considered significantly of about more than 0.86.

Keywords: Desertification; remote sensing; GIS; land cover/land use; Landsat satellite.

1. Introduction

Desertification is one of the biggest problems and phenomena that threaten arid and semi-arid environments (Li et al., 2022). It directly threatens animal and plant environments, and results in direct or indirect damages and dimensions on human social, economic, and political life, Desertification in Iraq, especially in the center and south, is quickly escalated, and great efforts have been made to identify and study its causes and effects. Recent studies from the Agriculture Directorate have indicated that the health and livelihood of more than one and a half billion people on Earth are threatened. More than 20% of the Earth's surface area, equivalent to about 30 million km^2, is directly affected by the danger. Soil productivity in an area estimated at 20,000 km^2 annually has reached the point of "zero economic productivity" (Tiffen & Mortimore, 2002).

In arid and semi-arid regions, satellite images and RS are crucial tools for tracking the processes of desertification and land degradation (Al-Timimi, 2021; Jasim, 2016). Agricultural production is also losing an estimated $26 billion per year. About 52% of the land used for agriculture is moderately or severely affected by soil degradation factors. The loss of agricultural land in recent decades represents thirty times the historical rate of land loss, as the world loses about 12 million hectares annually, equivalent to 23 hectares per minute. Desertification has threatened the future of hundreds of millions of people living in arid and semi-arid areas, which represent about 15% of the world's population. In general, about half of those affected by desertification are poor and extremely poor as a result of the scarcity of food caused by desertification.

The geographical concept of desertification is defined as a gradual decrease or total deterioration in the productive capacity of the soil, which leads to the environment acquiring new characteristics over time that resemble the characteristics of real deserts (Sayl et al., 2021; Thamer et al., 2024). There is desertification resulting from permanent (or emergency) drought and/or desertification resulting from human misuse of natural environmental resources. Another type of desertification results from the interaction of natural and human factors. All desertification types lead to disruption of the natural environmental balance. The degree of desertification danger is represented by its severity in a certain area and the extent of its danger to natural resources such as soil, water, and natural vegetation (Falih et al., 2023). This danger is determined according to the type of causes, whether natural or human factors or both (Sidiropoulos et al., 2021). United Nations has identified the desertification danger in three categories: very dangerous, dangerous, and medium-risk.

This problem has emerged in the study area as a result of several natural and human factors, most notably the dry and semi-dry climate of the region and the suboptimal investment of natural resources and wealth, which has had an impact on reducing the Earth's vital energy and disrupting the balance of the ecosystem. This picture has clearly appeared and worsened since the beginning of 2014 until the present time. A recent study conducted by Awadh (2024) concluded that significant environmental challenges, such as desertification, soil loss, and water scarcity, are currently plaguing Iraq (Awadh, 2024). Another study proved that Iraq is currently

experiencing severe droughts and dry spells, and an increase in the encroachment of sand dunes on agricultural land. In order to mitigate these negative effects, all of the countries in the region must work together and find solutions, not just at the local level (Adamo et al., 2022).

The combination of remote sensing techniques and GIS is considered one of the basic means for surveying and monitoring land cover and its resources and identifying their distribution and characteristics (Al-Quraishi & Negm, 2020; Fatah & Omar, 2023; Hason et al., 2022). Remote sensing data can provide the main sources of data to process and convert them into information efficiently and effectively, which traditional methods cannot provide (Almallah & Almulla, 2023). Since there is sufficient evidence of the effects of human activity and climate change processes on the environment, the growing rate of desertification on a worldwide scale is one of the most urgent issues for both environmental experts and the general public. In recent years, several definitions of desertification have been proposed, but the most common concept of desertification is not only related to climate change but also to changes caused by humans, especially those associated with inappropriate land use, such as overgrazing, agricultural intensification, and deforestation (Zwain et al., 2021). Thus, this research aims to conduct an assessment and evaluation of the LC of Al-Hay District, Wasit Governorate, Iraq, using remote sensing and GIS based on satellite imagery obtained from Landsat 8 for the years 2014 and 2022. Two factors were taken into account while selecting the years 2014 and 2022: data reliability and environmental significance. Significant drought events, increasing salinization, and modifications to irrigation practices occur throughout this time. Furthermore, the widespread availability of trustworthy and high-quality satellite imagery in 2014 made it feasible to accurately classify land cover and detect changes in it (Landsat 8, Sentinel-2).

2. Research Significance

This integration between RS and GIS is used in preparing plans and programs through which the desertification phenomenon can be confronted. The importance of this research lies in clarifying and highlighting the problem of desertification as one of the most significant issues in arid and semi-arid areas, including the study area. The present research discusses the effects of desertification in Al-Hay District in Wasit Governorate for the years from 2014 to 2022 using remote sensing by building land cover classification maps and detecting the main types of land cover and determining its importance and monitoring its changes based on digital processing of satellite images from Landsat 8. In addition to identifying desertification patterns within the study area, such as desertification of pasture lands or desertification of agricultural lands.

3. Study area

The area under study is located in the southern part of Wasit Governorate between latitudes 31°55' and 32°26' north and longitudes 45°36' and 46°21' east. The study area (Figure 1) is located specifically in Al-Hay district, Wasit Governorate, eastern Iraq. The area of Wasit Governorate is about 2208 km^2, which includes several districts: Al-Hay, Al-Haidariya, Al-Bashair, Al-Hurriya, and Al-Muwafaqiya as shown in Figure 1. The study area is bordered by

Al-Kut Center district to the north and east, Al-Numaniyah district to the northwest, Dhi Qar Governorate to the south, and Al-Diwaniyah Governorate to the southwest.
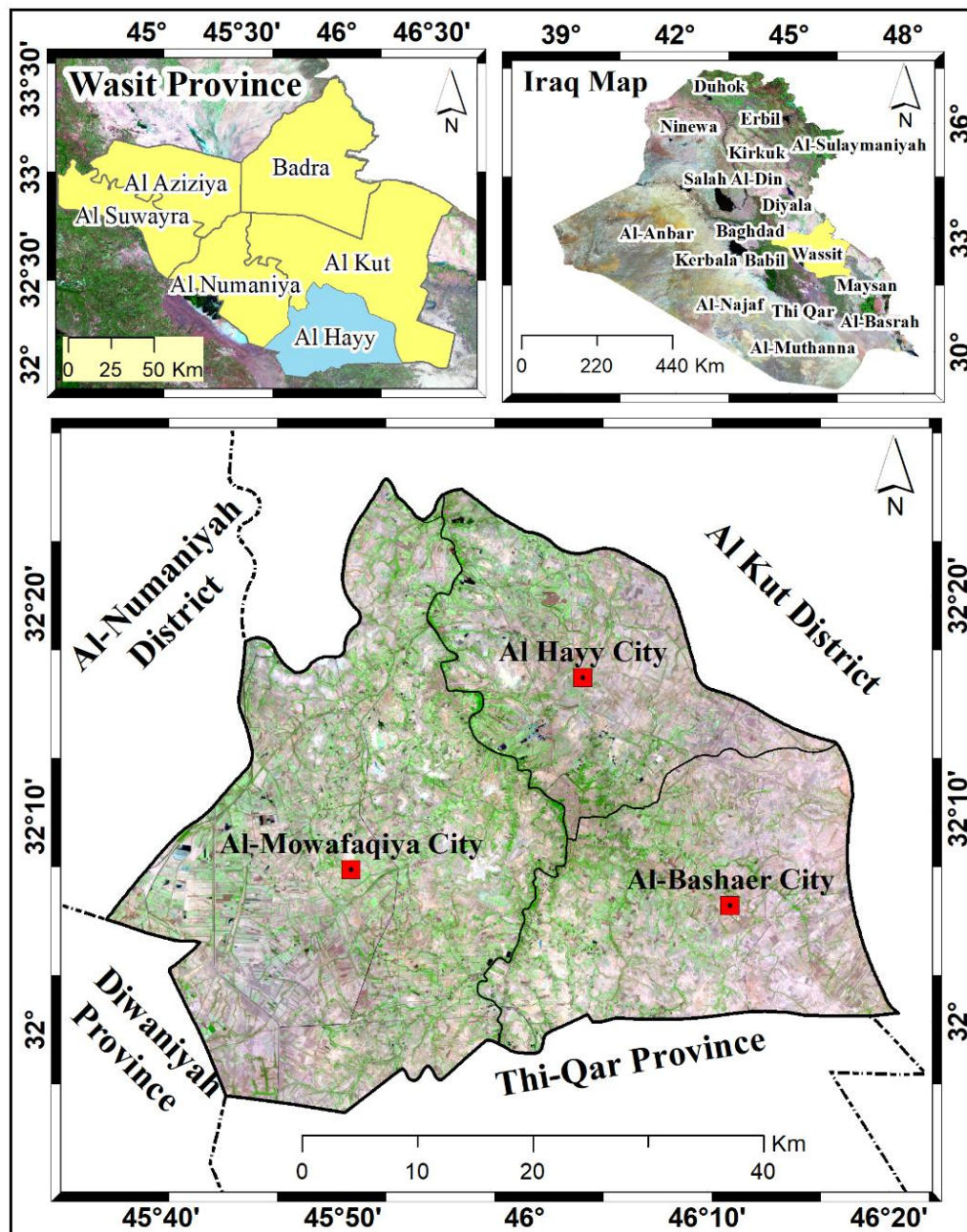

Figure 1. Spatial boundaries of the study area.

4. Methodology

The research methodology flow chart is shown in Figure 2. This research was implemented via two stages:

The first stage included preparing the data for the study area in terms of satellite imageries of 15 m to 30 m resolution. The images were chosen for two scenes for the Landsat 8 satellite and

the OLI (Operational Land Imager) sensor for the years 2014 and 2022 respectively for each of the paths (167 – 38). Table 1 shows the Landsat satellite image characteristics.

The second stage included several processes of merging the ranges, cutting out the study areas, and various improvement processes. Eventually, the satellite images were digitally analyzed and processed including separating the land covers from other unneeded areas. Then calculate their areas for the different years adopted in this study. Comparison of the results between the selected years and identifying the most important changes that occurred.

The reason behind choosing the years 2014 and 2022 due that two justifications were taken into consideration: environmental importance and data ratability. During this time, there are significant drought occurrences, rising salinization, and adjustments to irrigation techniques. Furthermore, accurate land cover classification and change detection became possible in 2014 with the widespread availability of reliable and high-quality satellite imagery (Landsat 8, Sentinel-2).
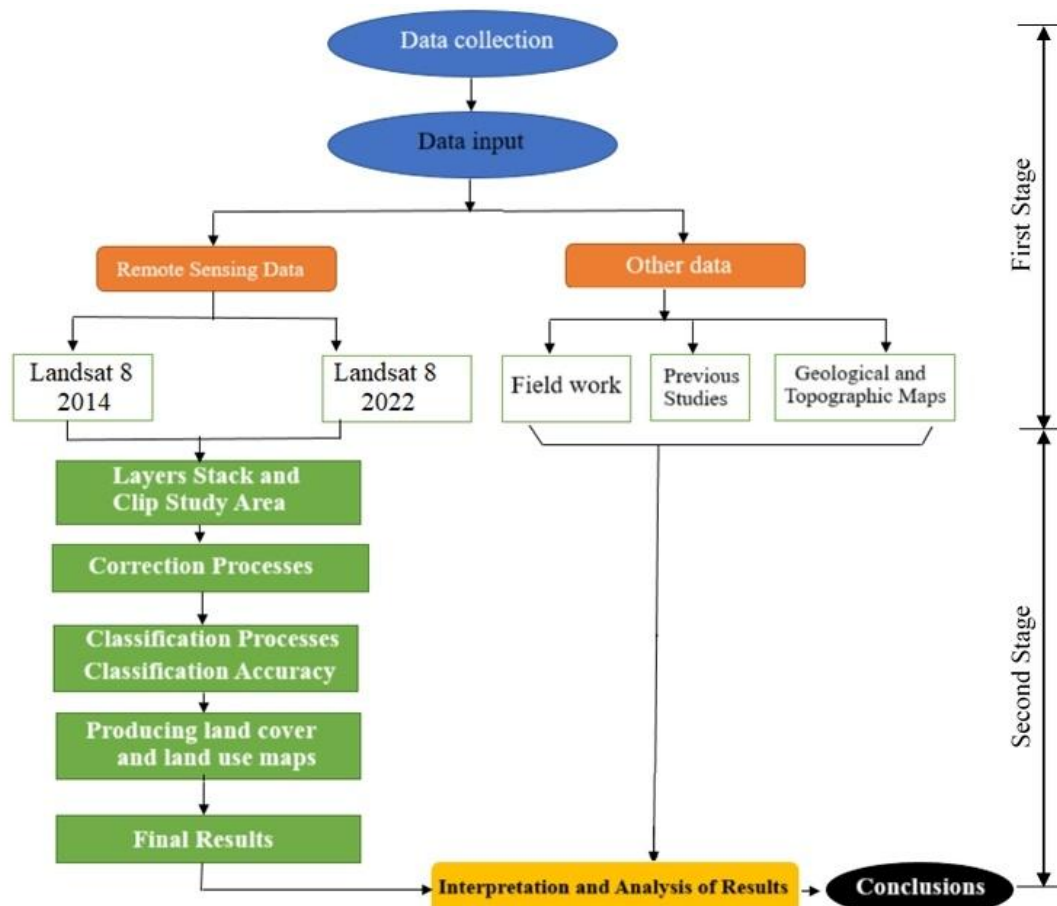

Figure 2. Adopted methodology in the present study.

Table 1. Landsat satellite image characteristics were used in the present study.

Year	Acquisition date	Satellite	Sensors	Path	Row	Bands used	Resolution (m)
2014	2014 July, 20	Landsat 8	OLI-1	167	38	1,2,3,4,5,6, and 7	30
2022	2022 July, 22	Landsat 8	OLI-1	167	38	1,2,3,4,5,6, and 7	30

4.1. Data collection

Landsat 8 satellite data was employed herein to obtain the satellite images. There were two scenes, one scene for the year 2014 on July 20 and another scene for the year 2022 on July 22. These satellite images were obtained from the USGS (https://earthexplorer.usgs.gov/) with the following details: Operational Land Imager device (OLI) sensor, Longitudinal path = 167, transverse path = 38, cloud cover = 0, and spatial resolution of (15 – 30) m. Note that the date of capturing all satellite images was at the beginning of summer, specifically June, so that the images are compatible and to get rid of the effect of different seasons and to obtain more accurate results. All Landsat 8 OLI satellite data characteristics and specifications can be found at https://www.usgs.gov/landsat-missions/landsat-8.

4.2. Classification

Visual classification is based on studying the digital data shown by various feature patterns based on their spectral reflection and emission characteristics (Li et al., 2022). Multispectral data is used in the visual classification process to convert visual data into information. Classification aims to place all visual cells in groups according to their homogeneity and similarity in the form of a classification map. The accuracy in producing such maps depends mainly on the accuracy of the classification process of the study.

There are two main methods for conducting the classification process: Supervised Classification and Unsupervised Classification (Maurício et al., 2023). Supervised classification (Figure 3) depends on testing small locations that are groups of homogeneous samples within the visualization based on maps and study fields, and thus, they represent the various land cover configurations. These samples refer to what are called training areas. Then each cell in the visual data set is placed in the land cover pattern closest to it spectrally. Unsupervised classification (Figure 3) shows unknown cells in the visualization and then groups them into rows based on the convergence of their numerical data (Damri et al., 2024). The classes resulting from this method are known as spectral classes, which are placed based on the clusters of spectral values within the visualization. The computer assigns the spectral reflectivity of each cell within the satellite image to a specific class of the specified classes, based on the raw data and its spectral values.

The algorithm of ISODATA was used for unsupervised classification because of its capability to cluster the image pixels deprived of earlier knowledge. This would help to differentiate between LC types. In supervised classification, the algorithm of MLC was employed due to its high accuracy and appropriateness to define the training samples.
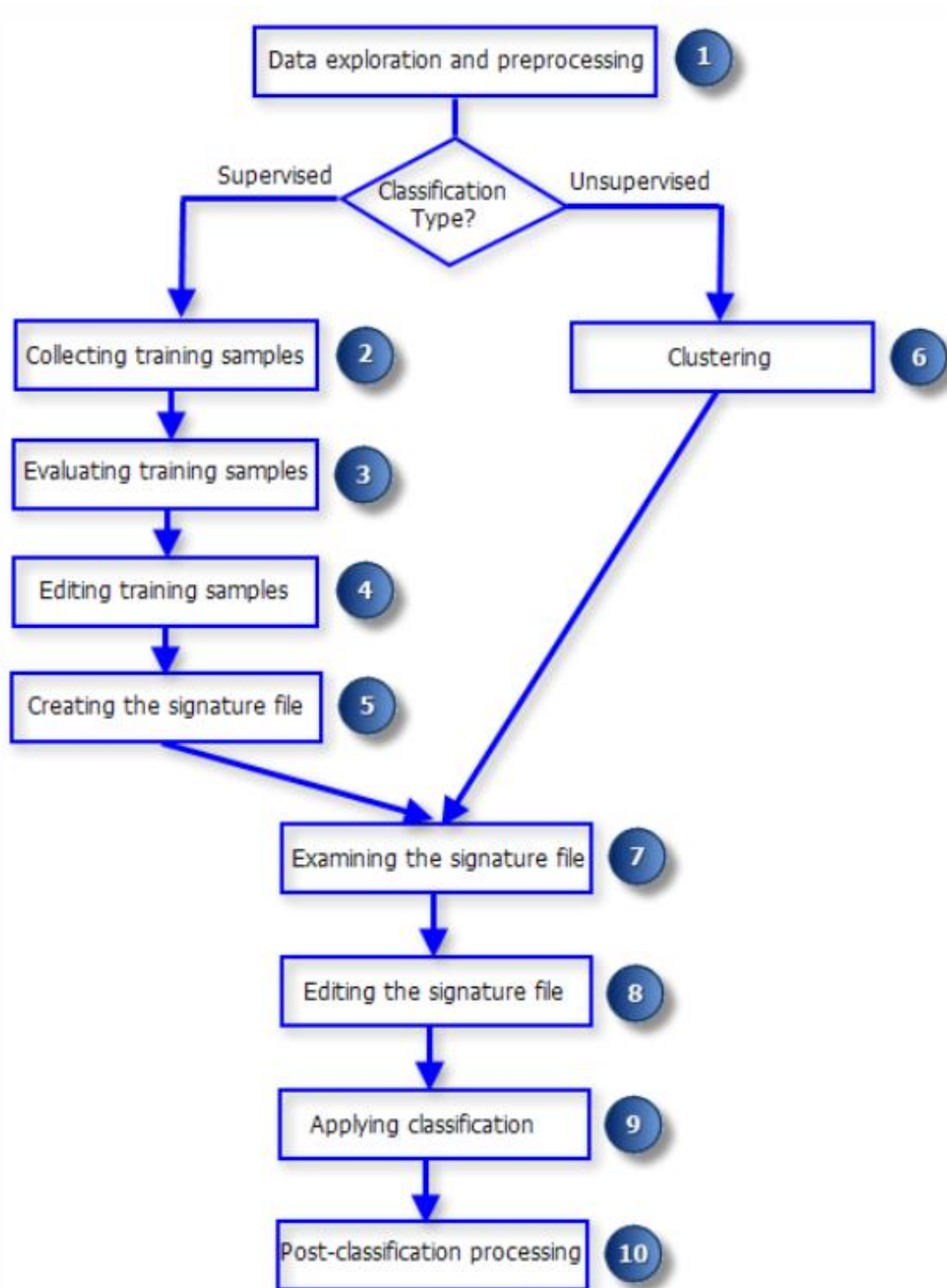
Figure 3. Image classification (arcgis.com).

4.3. Spectral signature behavior

The spectral signature can be defined as the pattern or behavior of ground features towards the electromagnetic spectrum in terms of absorption or reflection and is represented in the form of a graphic curve that reflects the amount of reflected or absorbed energy (Elachi & Van Zyl, 2021). The spectral behavior of different ground covers and their components is directed to

remote sensing information (Wang et al., 2023). Shepherd indicated that reflectivity as a function of wavelength gives basic features specific to different materials called spectral signatures. The spectral signature of ground features represents a collective characteristic derived from the internal spectral behavior of the components of those features and depends mainly on their physical and chemical properties and their interaction with the electromagnetic spectrum.

5. Results and discussion

5.1. Unsupervised classification

Adopting pre-analysis by unsupervised classification supports better design of training areas. In the meantime, the reason behind using both classification approaches (unsupervised and supervised) is to obtain more accurate, flexible, and stronger results data (James et al., 2023). Figure 4 and Figure 5 show the spatial and area distribution of six classes in an unsupervised manner for the years 2014 and 2022, respectively, using the satellite image of the Landsat 8 satellite and with a discriminating resolution of 30 meters for the multi-band image. ArcGIS software version 10.2 was employed herein. Table 2 represents the calculation of the area of each class and its percentage by multiplying the number of image elements (pixels) for each class by the area of one pixel (the area of one pixel for Landsat satellite images is 900 meters) and then dividing the result by the area of the total area and multiplying it by 100 to obtain its percentage.

According to Table 2, it can be noticed that there are classes that appeared isolated in the first image, while the same classes appeared to overlap with other classes in another image. It was also noticed that there is a variation in the area of the six classes for each of the 2014 and 2022 satellite images. The reason for this is the variation, like the distribution of classes in the two satellite images, as well as the difference in the climatic and temporal conditions prevailing during that period, in addition to the nature of land use. The reason behind classifying the study area into 6 classes is that (e.g., 3 – 4) classes may lead to merging the types of distinct areas. On the other hand, too many classes (e.g., 7 – 12) may create similar classes with no land differences. Thus, 6 classes hit a balance of enough variation with manageable interpretation.
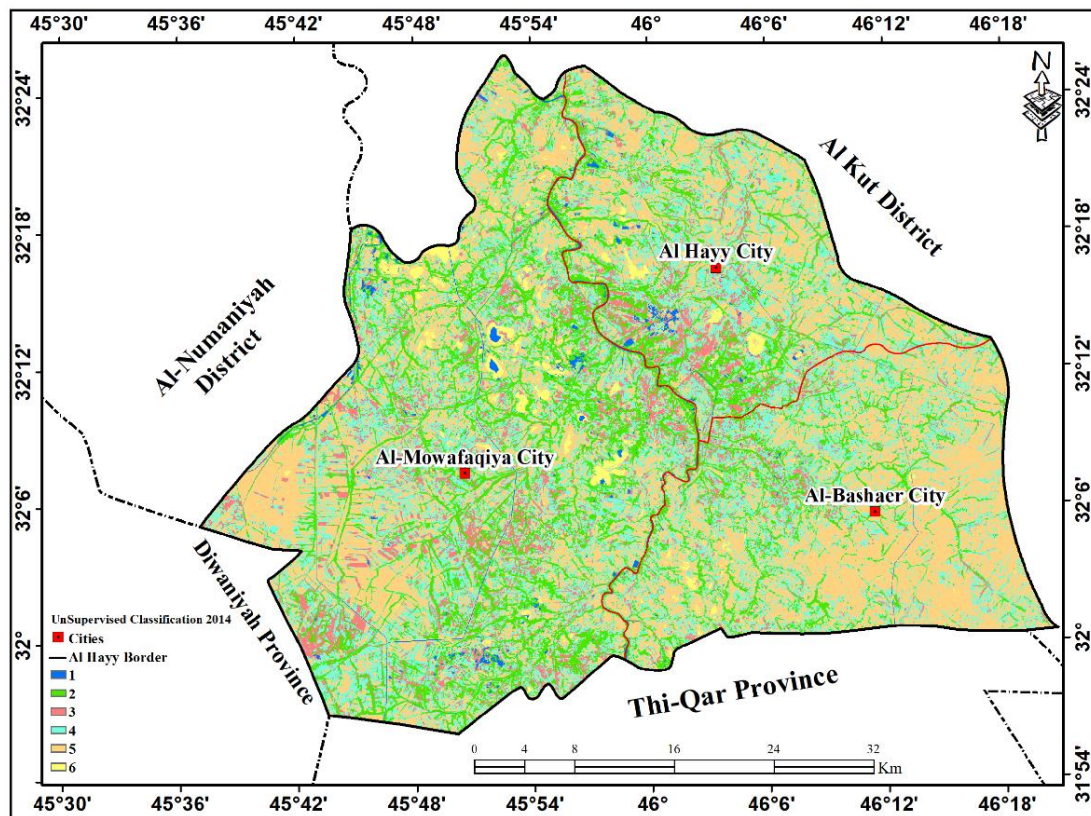
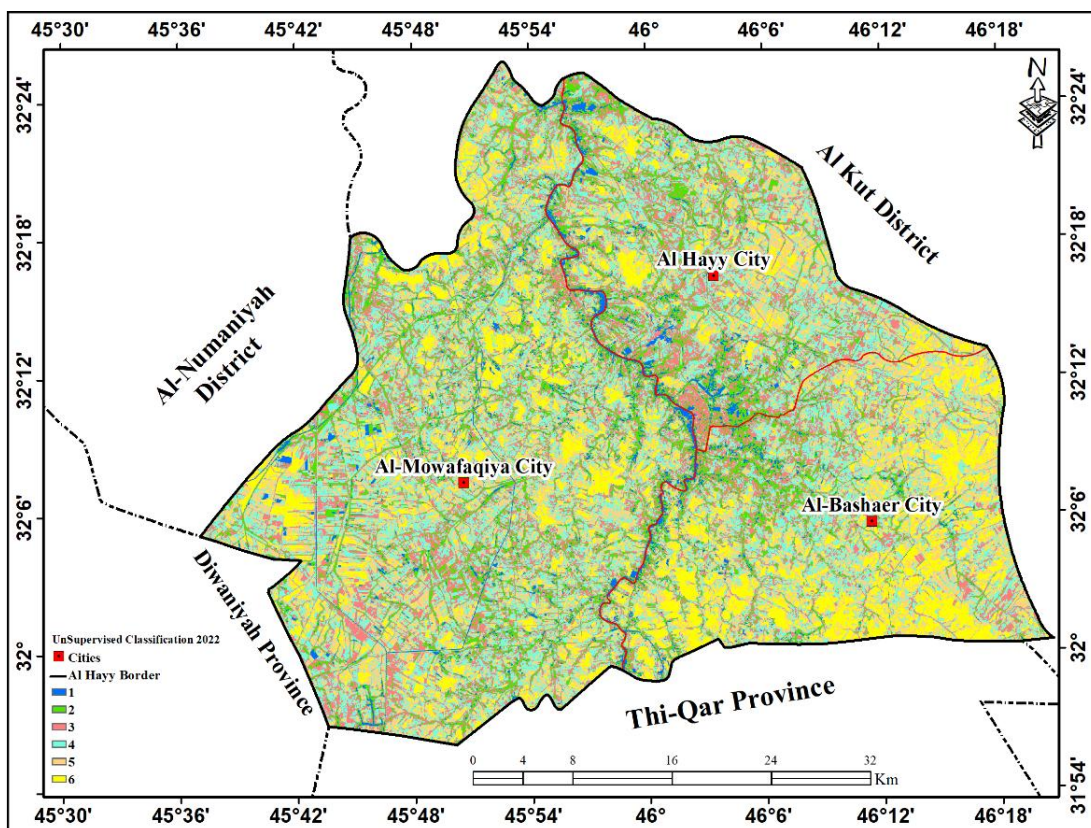**Figure 4.** Unsupervised classification map of the district (year 2014).

Figure 5. Unsupervised classification map of the district (year 2022).

Table 2. Details classifications of the six classes (2014 and 2022).

Class	Classification					
	2014			2022		
	Image element (No.)	Area (km^2)	%	Image element (No.)	Area (km^2)	%
1	29869	26.9	1.2	73459	66.1	3
2	433986	390.6	17.7	284532	256.1	11.6
3	218589	196.7	8.9	528133	475.3	21.5
4	730106	657.1	29.8	701407	631.3	28.6
5	998535	898.6	40.7	566114	509.5	23.1
6	43187	38.9	1.8	300627	270.5	12.2
Total		2208.7	100	Total	2208.7	100

5.2. Supervised classification

5.2.1. Land cover map interpretation

The classification process aims to place all the cells of the satellite image into groups according to their homogeneity and similarity in the form of maps through which the features and types of land cover are determined. Figure 6 shows the digital supervised classification map of the land cover of the study area for the year 2014 using the satellite image of the Landsat 8 with a distinctive resolution of 15 to 30 meters for each of the multi-band and panchromatic band images respectively. Figure 6 illustrates also the spatial and area distribution of six types of land cover and land uses in the Al-Hay District. The first rank was for the barren lands category with an area of 1545.67 km^2, which is about 70% of the total area of the study area. Most of this area was concentrated in the eastern region of the study area. As for the water bodies, their area reached 26.87 km^2, representing 1.2% of the area of the study area, and was represented by both the Tigris River and the associated watercourse. For the agricultural lands, their area was 393.20 km^2, representing 18%, which appears concentrated in the central region of the study area around and on the banks of the Tigris River and its various branches. The urban lands category reached 8.93 km^2, representing 0.4% of the area of the study area, and was represented by Al-Hay District and some cities and villages spread along the banks of the Tigris River. In the saline lands category, their area reached 38.59 km^2, representing 2% of the study area. Noting that all unknown pixels, overlapping pixels, or mixed pixels were classified as mixed land. This is due to many reasons, the most important of which is the presence of more than one class within a single pixel or the similarity in spectral signature to merge or overlap, especially between the barren land class and the urban land class. The spatial resolution of the satellite images used also affects the presence of mixed, unclassified, or unclassifiable pixels. Another reason is that the spatial resolution of the satellite (e.g., 30 meters for Landsat), and land parcels are diverse.
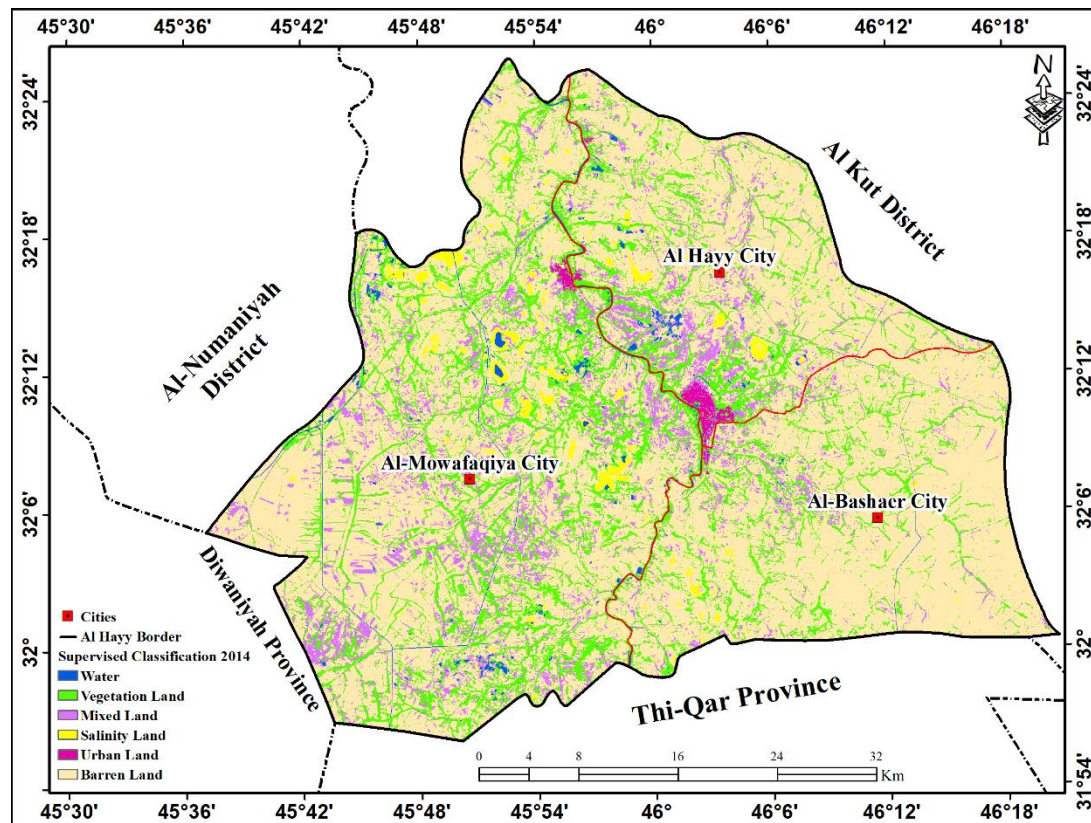
Figure 6. Supervised classification map (year 2014).

Figure 7 shows the digital classification map (LC/LU) for the current research area for the year 2022 using the Landsat 8 satellite image with a resolution of 30 and 15 meters for both the multi-band image and the panchromatic band, respectively. The map shows the spatial and area distribution of six (LC/LU) categories in Al-Hay District. In 2022, the barren land category still represents the largest proportion of the study area with about 69% of the total area of the study area with an area of 1515.50 km^2. As for the water bodies, their area amounted to 22.51 km^2 and 1% of the area of the research region. As for the agricultural lands, their area was 351.41 km^2 and 16%. As for the urban land category, its area amounted to 12.25 km^2 and 0.55% of the area of the research region. As for the saline land category, its area amounted to 116.38 km^2 and 5% of the area of the study area.
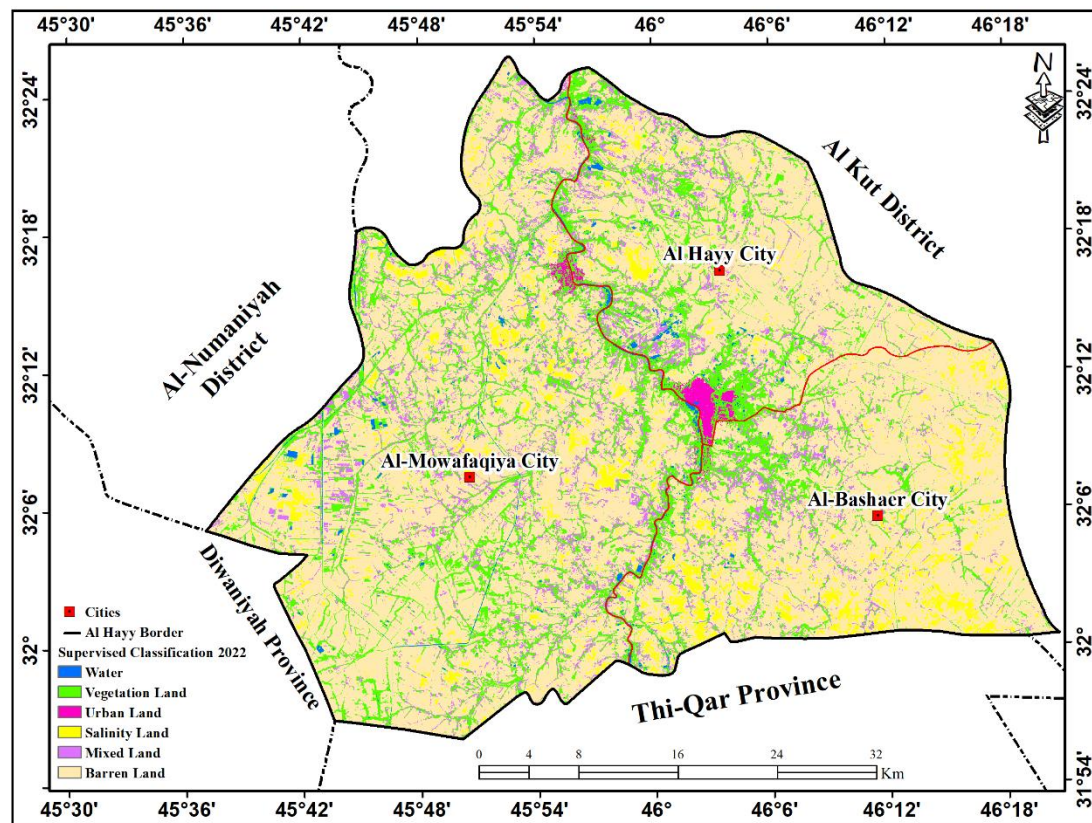
Figure 7. Supervised classification map (year 2022).

Table 3 shows a comparison of the area and percentage distribution for each of the main land cover and land use categories for the study area based on the results of the supervised classification for the years 2014 and 2022. It was noted that there was a decrease during the study period in the area of agricultural land, which decreased from 393.20 km^2 in 2014 to 351.41 km^2 in 2022 by about 41.79 km^2. This decrease in the area of agricultural land was accompanied by a significant increase in the area of saline land from 38.59 km^2 in 2014 to 116.38 km^2 in 2022 by about 77.78 km^2, which is a large area when compared to the total area of the study area. The researcher also noted that there was an increase during the study period in the area of urban land, which increased from 2014 to 2022 by about 3.3 km^2. Also, the area of the barren lands category decreased during the study period from 1545.67 km^2 in 2014 to about 1515.50 km^2 in 2022, i.e. a decrease of about 32 km^2. Figure 8 shows the percent of changes that occurred in the land cover of the study area in the year 2022 compared with 2014. Interestingly, the agricultural land decreased from 393.2 km^2 to 351.41 km^2 in 2014 and 2022, respectively. Similarly, the barren land also decreased from 1545.67 km^2 to 1515.5 km^2 in 2014 and 2022, respectively, despite it should be increased. This is might due to several explanations: (1) The increase in saline land from 38.59 km^2 in 2014 to 116.38 in 2022 resulted might in the degradation of the agricultural land into saline land, not barren land. (2) Some areas of barren land appeared as mixed land, which almost stayed the same (195.44 – 190.69) km^2, and this is common in supervised classification based on the used training sample.

Table 3. Area and percentage of LC/LU.

Color	Land Cover	2014		2022	
		Area (km^2)	**%**	**Area (km^2)**	**%**
[blue]	Water	26.87	1.2	22.51	1.02
[green]	Agriculture	393.2	17.8	351.41	15.91
[magenta]	Mixed	195.44	8.8	190.69	8.63
[yellow]	Urban	8.93	0.4	12.25	0.55
[violet]	Barren	1545.67	70	1515.5	68.62
[tan]	Saline	38.59	1.7	116.38	5.27
Total		2208.72	100	2208.73	100
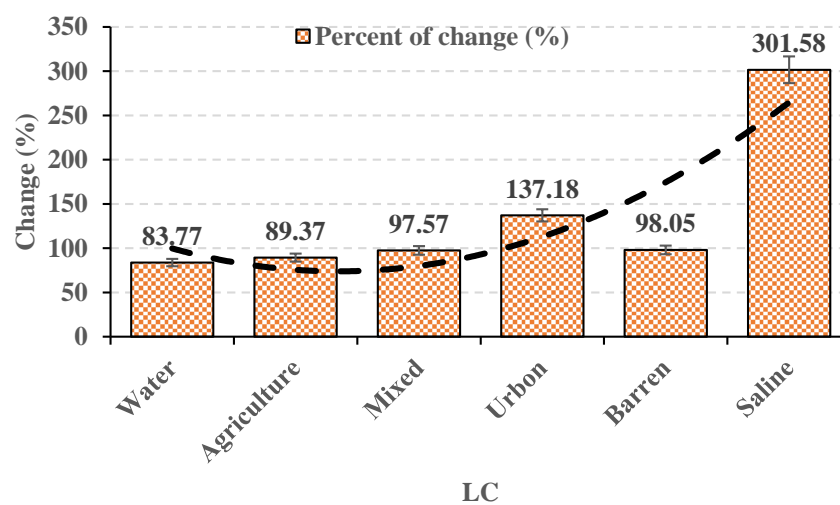
Figure 8. Percent of change (2014 vs. 2022).

5.3. Classification accuracy evaluation

Error matrices were an essential part of this study and have been employed in many land classification investigations. Additionally, the Kappa coefficient and error matrix are now commonly used to evaluate the accuracy of the classification of satellite images (Rwanga & Ndambuki, 2017). Thus, to evaluate the accuracy of the classification maps, 500 random reference data points were used for land cover and land use categories. The first 50 reference points were created through fieldwork carried out during different periods in 2021 and 2022 as shown in Figure 9. The other 450 reference points were created and distributed throughout the study area using the Creates Random Points tool for ArcGIS software and then manually classified according to cover type.

Table 4 and Table 5 illustrate the error matrix and accuracy evaluation results for the classified satellite images of the study area for the years 2014 and 2022, respectively. Moreover, in remote sensing categorization, it is typical for multiple land cover (LC) types to overlap, such as when agriculture is incorrectly labeled as mixed, urban, barren, or saline. This is particularly true

when employing medium-resolution Landsat data. In satellite images, several LC types may have comparable spectral signatures, particularly in reflectance bands that organization systems use. Table 6 shows the final results of the overall accuracy evaluation and Kappa coefficient for the study area classification maps.

Table 4. Error matrix and classification accuracy rating for the year 2014 image.

Land cover	Water	Agriculture	Mixed	Barren	Urban	Saline	Total	Accuracy
Water	59	0	0	0	0	1	60	98.33
Agriculture	0	81	3	2	3	3	92	88.04
Mixed	1	2	74	3	2	3	85	87.06
Barren	0	2	3	106	2	4	117	90.6
Urban	0	3	4	2	68	1	78	87.18
Saline	1	2	2	2	4	57	68	83.82
Total	61	90	86	115	79	69	445	
Accuracy	96.72	90	86.05	92.17	86.08	82.61		89

Table 5. Error matrix and classification accuracy rating for the year 2022 image.

Land cover	Water	Agriculture	Mixed	Barren	Urban	Saline	Total	Accuracy
Water	67	1	0	0	0	0	68	98.53
Agriculture	1	86	2	2	3	3	97	88.66
Mixed	1	4	81	2	2	2	92	88.04
Barren	0	3	3	94	1	2	103	91.26
Urban	0	3	5	2	54	0	64	84.38
Saline	0	2	2	3	3	66	76	86.84
Total	69	99	93	103	63	73	448	
Accuracy	97.1	86.87	87.1	91.26	85.71	90.41		89.6

Table 6. Accuracy classification.

Classified image	Total accuracy (%)	Kappa coefficient (K)
2014	86.00	0.80
2022	90.80	0.87

About 445 and 448 samples, respectively, of the total number of reference points for the error matrix for the supervised classification results for the years 2014 and 2022 were randomly selected and successfully classified. The number of random reference points that were incorrectly classified was 55 and 52 samples out of the total number of reference points for the error matrix for the directed classification results for the years 2014 and 2022, respectively. The four classification maps seem to exhibit close classification accuracies based on the classification accuracy results, which could be because the Landsat 8 satellite images are similar in terms of spatial, spectral, and radiometric resolution.

Figure 9. Field photographs of the study area from various views.

6. Research Limitation

A number of limitations should be noted, even if the study offers insightful information about the dynamics of desertification and changes in land cover in Al-Hayy District from 2014 to 2022. First, the detection of fine-scale features such as minor urban developments, fragmented vegetation patches, or narrow irrigation canals may be limited by the 30 m spatial resolution of Landsat data. Second, spectral similarities between some land cover types (such as saline and barren terrain) may impact classification accuracy, potentially resulting in misdiagnosis. Despite the use of both supervised and unsupervised classification techniques, the caliber and representativeness of the training data continue to influence how reliable the findings are.

7. Conclusions

A number of limitations should be noted, even if the study offers insightful information about the dynamics of desertification and changes in land cover in Al-Hayy District from 2014 to 2022. First, the detection of fine-scale features such as minor urban developments, fragmented vegetation patches, or narrow irrigation canals may be limited by the 30 m spatial resolution of Landsat data. Second, spectral similarities between some land cover types (such as saline and barren terrain) may impact classification accuracy, potentially resulting in misdiagnosis.

Despite the use of both supervised and unsupervised classification techniques, the caliber and representativeness of the training data continue to influence how reliable the findings are.

It is concluded that the problem of desertification is subject to natural and human factors, but human factors have an effective role in increasing this problem through synergy with natural factors, including climate change. The study proved that the use of integration between remote sensing techniques and geographic information systems is of great importance in monitoring the phenomenon of desertification.

It was noted that there was a decrease of the agricultural land from 393.20 km^2 in 2014 to 351.41 km^2 in 2022 by about 41.79 km^2. This decrease in the area of agricultural land was accompanied by a significant increase in the area of saline land from 38.59 km^2 in 2014 to 116.38 km^2 in 2022 by about 77.78 km^2. Besides, the urban land increased from 2014 to 2022 by about 3.3 km^2. However, the barren lands decreased from 1545.67 km^2 in 2014 to about 1515.50 km^2 in 2022, The convergence of the Landsat 8 satellite images in terms of spatial, spectral, and radiometric accuracy may be the reason why the four classification maps appear to exhibit close classification accuracy based on the classification accuracy results. For the years 2014 and 2022, the study's overall classification accuracy was 86% and 96%, respectively, and its Kappa coefficient was 0.8 and 0.87. Thus, the Kappa coefficient is deemed significant, and hence, the categorized image is deemed suitable for more study.

It is recommended to create a long-term monitoring program utilizing GIS and remote sensing to evaluate different changes such as the transition of LC, saline in soil, and NDVI trends. Additional studies are desirable to perform the classification accuracy assessment of the LC/LU of the study area using numerous new creative approaches. Furthermore, for yearly evaluations, use multi-temporal satellite data such as Sentinel-2 and Landsat 8 – 9.

Acknowledgments

References

Adamo, N., Al-Ansari, N., Sissakian, V., Jehad Fahmi, K., & Ali Abed, S. (2022). Climate Change: Droughts and Increasing Desertification in the Middle East, with Special Reference to Iraq. *Engineering*, *14*(7), 235–273. https://doi.org/10.4236/eng.2022.147021

Al-Quraishi, A. M. F., & Negm, A. M. (2020). Introduction to "Environmental Remote Sensing and GIS in Iraq" BT - Environmental Remote Sensing and GIS in Iraq. In A. M. F. Al-Quraishi & A. M. Negm (Eds.), *Springer Water ((SPWA))* (pp. 3–15). Springer International Publishing. https://doi.org/10.1007/978-3-030-21344-2_1

Al-Timimi, Y. K. (2021). Monitoring desertification in some regions of Iraq using GIS techniques. *Iraqi Journal of Agricultural Sciences*, *52*(3), 620–625. https://doi.org/10.36103/ijas.v52i3.1351

Almallah, I., & Almulla, S. (2023). Mapping Ground Water Potential Recharge Zones of Wadi Al-Batin Alluvial Fan, Using Remote Sensing and GIS Techniques, Southwestern Iraq. *Iraqi Bulletin of Geology and Mining*, *19*(1), 99–115. https://doi.org/10.59150/ibgm1901a07

Awadh, S. M. (2024). *Drought and Desertification Hazard in Iraq BT - Environmental Hazards in the Arabian Gulf Region: Assessments and Solutions* (pp. 377–395). Springer Nature Switzerland. https://doi.org/10.1007/978-3-031-71836-6_14

Damri, A., Last, M., & Cohen, N. (2024). Towards efficient image-based representation of tabular data. *Neural*

Computing and Applications, *36*(2), 1023–1043.

Elachi, C., & Van Zyl, J. J. (2021). *Introduction to the physics and techniques of remote sensing*. John Wiley & Sons.

Falih, A., Mohammed, A., Nada, K., Al Maliki, A., Jasm, A., Mahmood, A., & Abed, Z. (2023). Preparing Environmental Isotopes Databases for Determining Groundwater and Surface Water Relationships in Iraq. *Iraqi Bulletin of Geology and Mining*, *19*(2), 125–139. https://doi.org/10.59150/ibgm1902a09

Fatah, K., & Omar, A. A. (2023). Determination of Surface Roughness of the Land Texture Using Remote Sensing Data and Geo-Informatic Techniques: A Case Study in Kurdistan Region-Iraq. *Iraqi Bulletin of Geology and Mining*, *19*(1), 61–75. https://doi.org/10.59150/ibgm1901a05

Hason, M. M., Al-Sulttani, A. O., & Jasim, A. A. (2022). Performance evaluation of coronavirus closure on air quality over central, southern and northern parts of Iraq. *Journal of Environmental Engineering and Science*, *17*(4), 184–197. https://doi.org/10.1680/jenes.21.00039

James, G., Witten, D., Hastie, T., Tibshirani, R., & Taylor, J. (2023). *Unsupervised Learning BT - An Introduction to Statistical Learning: with Applications in Python* (G. James, D. Witten, T. Hastie, R. Tibshirani, & J. Taylor (eds.); pp. 503–556). Springer International Publishing. https://doi.org/10.1007/978-3-031-38747-0_12

Jasim, A. A. (2016). *Application of GIS Technique to Assess the Habbaniya Lake Water for Human Consumption*. *16*(1), 75–81. https://doi.org/10.37652/juaps.2022.174843

Li, P., Chen, P., Shen, J., Deng, W., Kang, X., Wang, G., & Zhou, S. (2022). Dynamic monitoring of desertification in Ningdong based on Landsat images and machine learning. *Sustainability*, *14*(12), 7470. https://doi.org/10.3390/su14127470

Maurício, J., Domingues, I., & Bernardino, J. (2023). Comparing vision transformers and convolutional neural networks for image classification: A literature review. *Applied Sciences*, *13*(9), 5521. https://doi.org/10.3390/app13095521

Rwanga, S. S., & Ndambuki, J. M. (2017). Accuracy assessment of land use/land cover classification using remote sensing and GIS. *International Journal of Geosciences*, *8*(04), 611.

Sayl, K. N., Sulaiman, S. O., Kamel, A. H., Muhammad, N. S., Abdullah, J., & Al-Ansari, N. (2021). Minimizing the impacts of desertification in an arid region: a case study of the West Desert of Iraq. *Advances in Civil Engineering*, *2021*(1), 5580286. https://doi.org/10.1155/2021/5580286

Sidiropoulos, P., Dalezios, N. R., Loukas, A., Mylopoulos, N., Spiliotopoulos, M., Faraslis, I. N., Alpanakis, N., & Sakellariou, S. (2021). Quantitative classification of desertification severity for degraded aquifer based on remotely sensed drought assessment. *Hydrology*, *8*(1), 47.

Thamer, F. M., Alhadithi, A. A., & Alaraji, A. A. (2024). Morphotectonic of Euphrates River between Al-Qaim and Haditha cities, western Iraq. *IOP Conference Series: Earth and Environmental Science*, *1300*(1), 12042. https://doi.org/0.1088/1755-1315/1300/1/012042

Tiffen, M., & Mortimore, M. (2002). Questioning desertification in dryland sub–Saharan Africa. *Natural Resources Forum*, *26*(3), 218–233. https://doi.org/https://doi.org/10.1111/0165-0203.t01-1-00023

Wang, J., Zhen, J., Hu, W., Chen, S., Lizaga, I., Zeraatpisheh, M., & Yang, X. (2023). Remote sensing of soil degradation: Progress and perspective. *International Soil and Water Conservation Research*, *11*(3), 429–454. https://doi.org/10.1016/j.iswcr.2023.03.002

Zwain, F. A., Al-Samarrai, T. T., & Al-Saady, Y. I. (2021). A study of desertification using remote sensing techniques in Basra Governorate, south Iraq. *Iraqi Journal of Science*, 912–926. https://doi.org/10.24996/ijs.2021.62.3.22